



Construction of a nomogram model for predicting peritoneal metastasis in gastric cancer: focused on cardiophrenic angle lymph node features

Xiaolong Gu¹ · Yang Li¹ · Gaofeng Shi¹ · Li Yang¹ · Hui Feng¹ · Yang Yang² · Zhidong Zhang³

Received: 7 November 2022 / Revised: 4 February 2023 / Accepted: 6 February 2023 / Published online: 18 February 2023
© The Author(s) 2023

Abstract

Background A different treatment was used when peritoneal metastases (PM) occurred in patients with gastric cancer (GC). Certain cancers' peritoneal metastasis could be predicted by the cardiophrenic angle lymph node (CALN). This study aimed to establish a predictive model for PM of gastric cancer based on the CALN.

Methods Our center retrospectively analyzed all GC patients between January 2017 and October 2019. Pre-surgery computed tomography (CT) scans were performed on all patients. The clinicopathological and CALN features were recorded. PM risk factors were identified via univariate and multivariate logistic regression analyses. The receiver operator characteristic (ROC) curves were generated using these CALN values. Using the calibration plot, the model fit was assessed. A decision curve analysis (DCA) was conducted to assess the clinical utility.

Results 126 of 483 (26.1%) patients were confirmed as having peritoneal metastasis. These relevant factors were associated with PM: age, sex, T stage, N stage, enlarged retroperitoneal lymph nodes (ERLN), CALN, the long diameter of the largest CALN (LD of LCALN), the short diameter of the largest CALN (SD of LCALN), and the number of CALNs (N of CALNs). The multivariate analysis illustrated that the LD of LCALN (OR = 2.752, $p < 0.001$) was PM's independent risk factor in GC patients. The area under the curve (AUC) of the model was 0.907 (95% CI 0.872–0.941), demonstrating good performance in the predictive value of PM. There is excellent calibration evident from the calibration plot, which is close to the diagonal. The DCA was presented for the nomogram.

Conclusion CALN could predict gastric cancer peritoneal metastasis. The model in this study provided a powerful predictive tool for determining PM in GC patients and helping clinicians allocate treatment.

Keywords Cardiophrenic angle · Lymph node · Gastric cancer · Peritoneal metastasis · Prediction nomogram

Introduction

On a global scale, gastric cancer (GC) ranked second in terms of mortality [1]. There was a 53% to 66% prevalence of peritoneal metastasis (PM) among patients with distant metastatic GC [2]. The quality of life of patients

with PM was not satisfactory. Gastric cancer patients with PM should first receive neoadjuvant chemotherapy instead of direct surgical resection. At present, intraperitoneal hyperthermic perfusion chemotherapy had also been proven to help improve the prognosis. Immunotherapy and targeted therapy were also the frontier directions of current research. Accurate PM prediction was crucial. According to the direct signs of peritoneal metastasis, a new scoring system was developed to evaluate gastric cancer peritoneal metastasis [3]. Previous studies had constructed nomograms that include the collagen signature and tumor clinicopathological features to predict peritoneal metastasis [4]. Some studies had developed partial imaging models to predict peritoneal metastasis [5–8]. Deep learning models or machine learning models were also used to predict PM [9, 10]. In terms of different means of image examination,

✉ Hui Feng
huifeng20151108@163.com

¹ Department of Radiology, The Fourth Hospital of Hebei Medical University, Shijiazhuang 050000, Hebei, PR China

² Department of Reproductive Medicine, The Second Hospital of Hebei Medical University, Shijiazhuang 050000, China

³ The Third Department of Surgery, The Fourth Hospital of Hebei Medical University, Shijiazhuang 050000, China

there was limited evidence about the effectiveness of magnetic resonance imaging (MRI) for gastric cancer staging [11–13]. On the other hand, positron emission tomography/ computed tomography (PET/CT) focused on the prediction of peritoneal metastasis based on new imaging agents or PET/CT imaging [14, 15]. However, the PET/CT examination was expensive and radioactive. In recent years, it had become not only necessary to predict the state of primitive cancer but also to pay attention to the risk factors of peritoneal metastasis after cure surgery [16].

Computed tomography (CT) was a regular noninvasive method of tumor node metastasis (TNM) staging. The typical signs of a diagnosis of PM were thickening of peritoneal cakes and massive ascites after excluding other diseases. These signs have high specificity but low sensitivity. However, the cases of gastric cancer with peritoneal metastasis without typical signs were confirmed to have small metastatic nodules after diagnostic laparoscopic exploration and could exist in isolation. Therefore, other methods were needed to judge the status of PM. The cardiophrenic angle lymph node (CALN) was effective in predicting rectal and ovarian cancer peritoneal metastasis [17, 18]. Especially for ovarian cancer, the cardiophrenic angle lymph nodes showed predictive value in diagnosis and prognosis [19–21]. Moreover, CT scanning of cardiophrenic lymph nodes could be performed at the same time as routine abdominal CT

scanning, without the need to book additional examinations again. There was a lack of a PM model for GC patients that focused on the CALN [22].

Accurate preoperative prediction of PM had clinical significance for the accurate selection of a treatment plan. This study aimed to establish a predictive model of gastric cancer peritoneal metastasis focusing on cardiophrenic lymph nodes.

Methods

Patient population and study design

The ethics committee approved this retrospective study (protocol number 2021KY120). As this was a retrospective study using deidentified data, written informed consent was waived. Our center retrospectively analyzed all GC patients between January 2017 and October 2019. The inclusion criteria were: [1] GC confirmed by pathology; [2] within two weeks before surgery, a CT scan was performed; [3] the status of PM was confirmed by surgery. The exclusion criteria were (Fig. 1): [1] prior anticancer therapy; [2] insufficient clinical data or CT images; and [3] patients with another cancer.

Fig. 1 Flowchart of the study

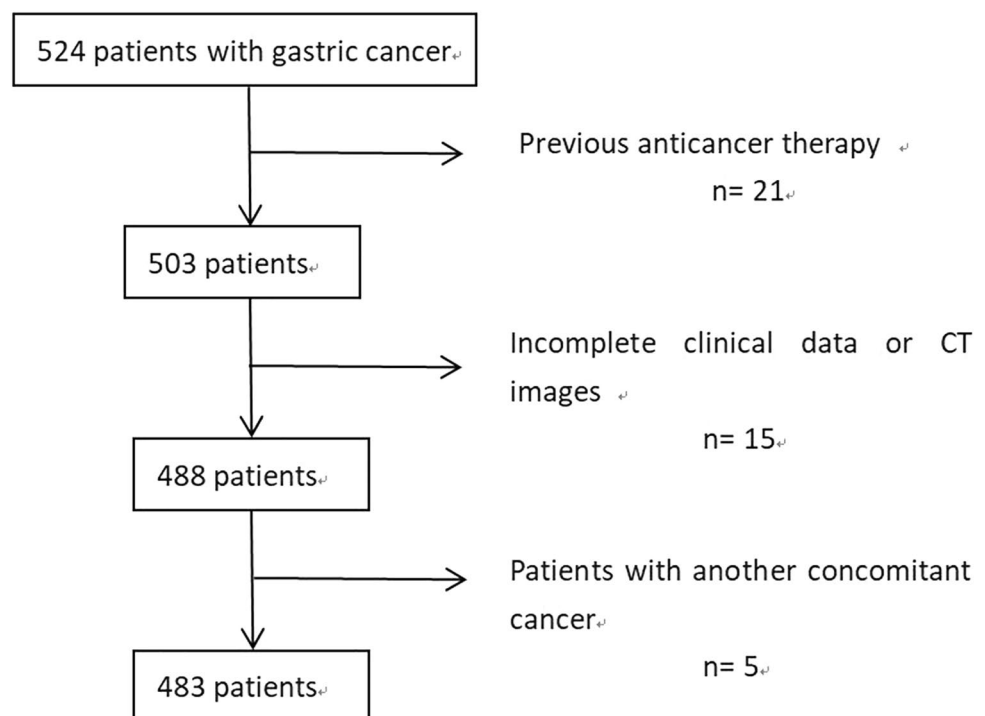


Table 1 Demographic and clinical characteristics of the study population

		All (N = 483)	Negative (N = 357)	Positive (N = 126)	p-value
Sex, N(%)	Male	347(71.8)	267(74.8)	80(63.5)	0.015
	Female	136(28.2)	90(25.2)	46(36.5)	
Location, N(%)	Cardia	68(14.1)	53(14.8)	15(11.9)	0.157
	Fundus	14(2.9)	13(3.6)	1(0.8)	
	Body	162(33.5)	112(31.4)	50(39.7)	
	Antrum	239(49.4)	179(50.1)	60(47.6)	
T stage, N(%)	T1–3	63(13.0)	55(15.4)	8(6.3)	0.009
	T4	420(87.0)	302(84.6)	118(93.7)	
N stage, N(%)	N0	97(20.1)	83(23.2)	14(11.1)	0.005
	N1	132(27.3)	100(28.0)	32(25.4)	
	N2	154(31.9)	110(30.8)	44(34.9)	
	N3	100(20.7)	64(17.9)	36(28.6)	
LM, N(%)	Negative	456(94.4)	337(94.4)	119(94.4)	0.984
	Positive	27(5.6)	20(5.6)	7(5.6)	
ERLN, N(%)	Negative	435(90.1)	333(93.3)	102(81.0)	< 0.001
	Positive	48(9.9)	24(6.7)	24(19.0)	
ELSFLD, N(%)	Negative	477(98.8)	353(98.9)	124(98.4)	0.684
	Positive	6(1.2)	4(1.1)	2(1.6)	
CALN, N(%)	Negative	242(50.1)	228(63.9)	14(11.1)	< 0.001
	Positive	241(49.9)	129(36.1)	112(88.9)	
SD of LCALN, median[IQR]	–	0.0[0.0,3.0]	0.0[0.0,2.0]	3.0[2.0,4.0]	< 0.001
LD of LCALN, median[IQR]	–	0.0[0.0,5.0]	0.0[0.0,4.0]	6.0[4.0,7.0]	< 0.001
N of CALNs, median[IQR]	–	0.0[0.0,1.0]	0.0[0.0,1.0]	1.0[1.0,2.0]	< 0.001
Age, median[IQR]	–	61.0[54.0,67.0]	61.0[55.0,68.0]	60.0[54.0,66.0]	0.031

LM liver metastasis, ERLN, enlarged retroperitoneal lymph nodes, ELSFLD enlarged lymph node in the left supraclavicular fossa, CALN cardiophrenic angle lymph node, SD of LCALN the short diameter of the largest CALN, LD of LCALN the long diameter of the largest CALN, N of CALNs the number of CALNs, IQR interquartile range

The clinical evaluation index

The clinical characteristics were recorded: age, sex, location, liver metastasis (LM), enlarged retroperitoneal lymph nodes (ERLN), enlarged lymph node in the left supraclavicular fossa (ELSFLD), T stage, N stage, and peritoneum metastasis (PM). Clinical staging was used in the T stage and the N stage. For ERLN and ELSFLD, we define that the short diameter was greater than 10 mm. The diameters were measured on the horizontal section CT images.

CT acquisition technique

All CT examinations were performed using one of three multidetector CT scanners: a 256-detector CT scanner (Revolution CT, GE Medical Systems) and two 128-detector CT scanners (SOMATOM Definition Flash, Siemens Healthcare, and Brilliance iCT, Philips Healthcare). The scans included unenhanced chest scans and multiphase contrast-enhanced abdominal scans to cover the cardiophrenic angle. The arterial phase and venous phase were scanned at 25 s and 70 s after injection. An automatic milliamper second technology was used to measure tube current while voltage was 120 kV. The reconstruction thickness was 1.0 mm because the measurement target is at the millimeter level.

Table 2 Logistic regression analysis of the risk factors for peritoneal metastasis

	Number	OR	95%CI	p-value
N of CALNs	483	4.89	[3.49,6.85]	0
LD of LCALN	483	1.92	[1.69,2.17]	0
SD of LCALN	483	2.48	[2.08,2.95]	0
Age				
≤ 60y	204			
> 60y	279	0.81	[0.54,1.22]	0.316
Sex				
Male	347			
Female	136	1.71	[1.11,2.63]	0.016
Location				
Cardia	68			
Fundus	14	0.27	[0.03,2.25]	0.227
Body	162	1.58	[0.81,3.06]	0.178
Antrum	239	1.18	[0.62,2.25]	0.606
T stage				
T1-3	63			
T4	420	2.69	[1.24,5.81]	0.012
N stage				
N0	97			
N1	132	1.90	[0.95,3.79]	0.07
N2	154	2.37	[1.22,4.61]	0.011
N3	100	3.34	[1.66,6.70]	0.001
LM				
Negative	456			
Positive	27	0.99	[0.41,2.40]	0.984
ERLN				
Negative	435			
Positive	48	3.27	[1.78,6.00]	0
ELSFLD				
Negative	477			
Positive	6	1.42	[0.26,7.87]	0.686
CALN				
Negative	242			
Positive	241	14.14	[7.79,25.66]	0

LM liver metastasis, ERLN enlarged retroperitoneal lymph nodes, ELSFLD enlarged lymph node in the left supraclavicular fossa, CALN cardiophrenic angle lymph node, SD of LCALN the short diameter of the largest CALN, LD of LCALN the long diameter of the largest CALN, N of CALNs the number of CALNs, OR odds ratio, CI confidence interval

Image analysis

Two radiologists (GXL has 7 years of experience in abdominal radiology, while YL has 19 years) retrospectively

analyzed the CALN independently. Disagreements were resolved through consensus. CT features on the entire cohort were recorded: [1] the presence of CALN, the long diameter of the largest CALN (LD of LCALN), the short diameter of the largest CALN (SD of LCALN), and the number of CALNs (N of CALNs); and [2] the presence of peritoneal carcinoma signs. PM status was blinded to the radiologist.

Statistical analysis

Chi-square or Mann–Whitney U tests were used to compare groups. $P < 0.05$ indicated statistical significance. PM risk factors were identified via univariate and multivariate logistic regression analyses. The receiver operator characteristic (ROC) curves were generated using these CALN values. Using the calibration plot, the model fit was assessed. A decision curve analysis (DCA) was conducted to assess the clinical utility. All statistical analyses were performed using R version 3.6.3 and Python version 3.7.

Results

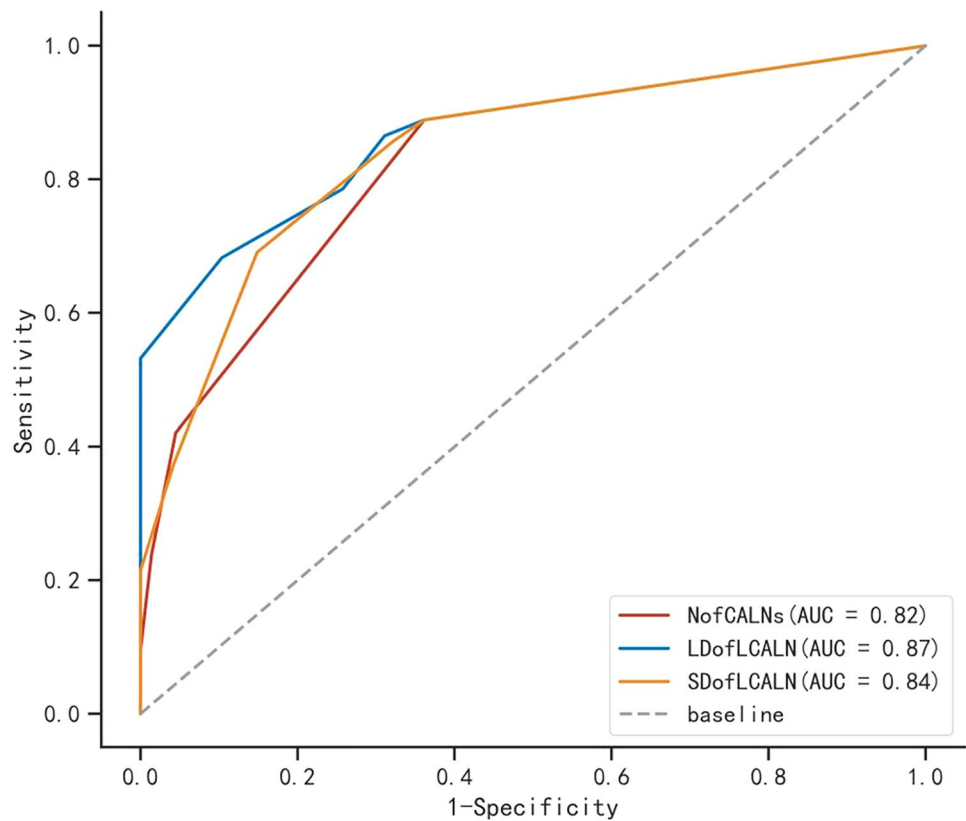
Patient characteristics

For peritoneal metastasis, 126 of 483 (26.1%) patients were positive while 357 patients were negative (Table 1). Study participants had an average age of 61 years.

Univariate and multivariate analysis for PM

For CALN, 241 of 483 (49.9%) patients were positive while 242 patients were negative. For ERLN, 48 of 483 (9.9%) patients were positive while 435 patients were negative. For ELSFLD, 6 of 483 (1.2%) patients were positive while 477 patients were negative. According to univariate logistic regression analysis (Table 1 and Table 2), the following relevant factors were associated with PM ($p < 0.05$): age, sex, T stage, N stage, ERLN, CALN, SD of LCALN, LD of LCALN, and N of CALNs. The multivariate analysis illustrated that the LD of LCALN (OR = 2.752, $p < 0.001$) and sex (OR = 2.663, $p = 0.004$) were PM's independent risk factors in GC patients (Supplementary Table 2).

Fig. 2 Receiver operating curve (ROC) curves of the risk factors. *CALN* cardiophrenic angle lymph node, *NofCALNs* the number of CALNs, *LDofLCALN* the long diameter of the largest CALN, *SDofLCALN* the short diameter of the largest CALN



ROC curve of risk factors

A correlation was determined between PM risk and CALN features (N of CALNs, LD of LCALNs, and SD of LCALNs) in GC patients using ROC curves (Fig. 2). The area under the curve (AUC), specificity, and sensitivity values were presented in Supplementary Table 1.

Multivariate predictive model and nomogram for predicting PM of GC

The AUC of the model was 0.907 (95% CI: 0.872–0.941), demonstrating good performance in the predictive value of PM (Fig. 3) (Supplementary Table 2).

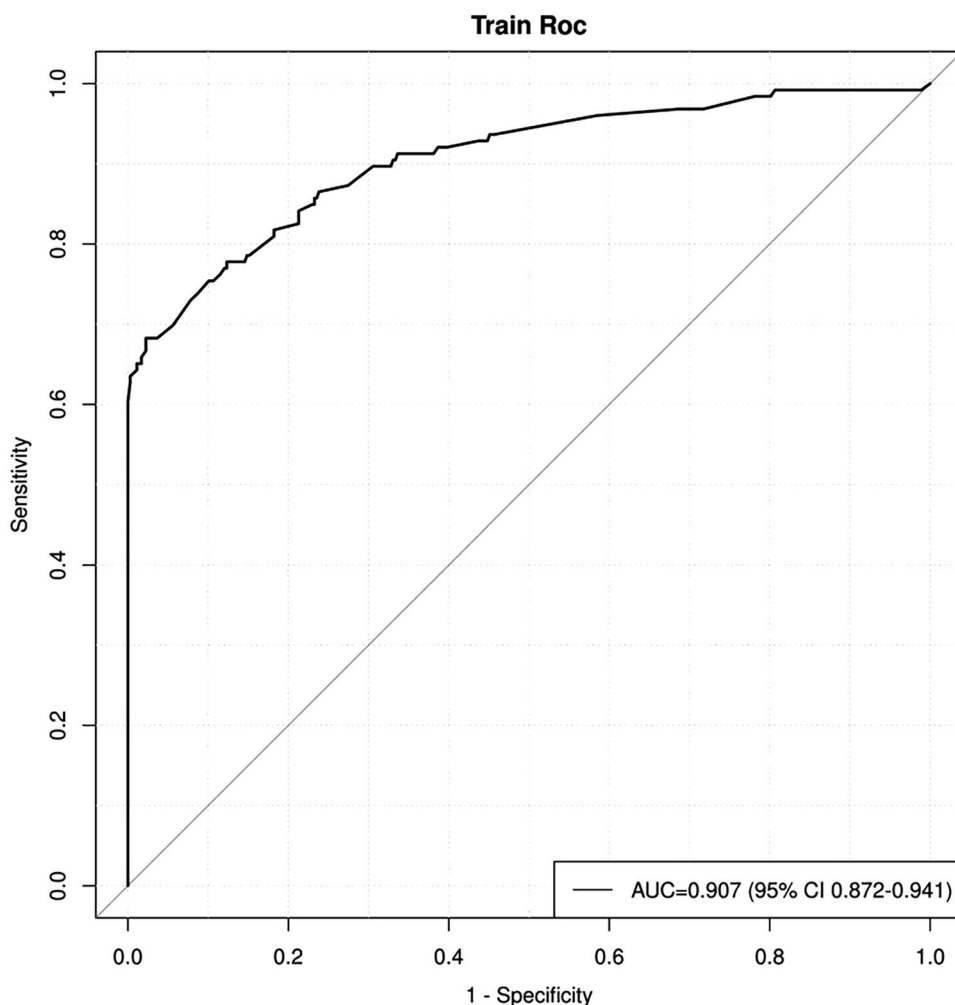
The nomogram of PM incidence was constructed (Fig. 4). There is excellent calibration evident from the calibration plot (Fig. 5), which is close to the diagonal. The DCA (Fig. 6) was presented to indicate that the model was clinically beneficial.

Discussion

CT was a regular method to diagnose PM of GC. The value of CALN in the prediction of PM has been continuously revealed. Our research found that combining CT with clinical factors could be used to create a predictive model.

We studied the value of clinicopathological features and CALN features as markers of GC with PM. Multivariate logical regression analysis showed that the long diameter of the largest CALN was an independent risk factor. Nomograph provided visual data information. A nomogram based on clinicopathological factors (sex, T stage, N stage) and CT signs of CALN (N of CALNs, LD of LCALN, CALN) could predict PM. There is excellent calibration evident from the calibration plot. The model was clinically beneficial by DCA. The nomogram in this study could accurately predict PM status in CG patients

Fig. 3 Receiver operating curve (ROC) curves of the multivariate logistic regression model. NofCALNs, number of CALNs; AUC, area under the curve; CI, confidence interval



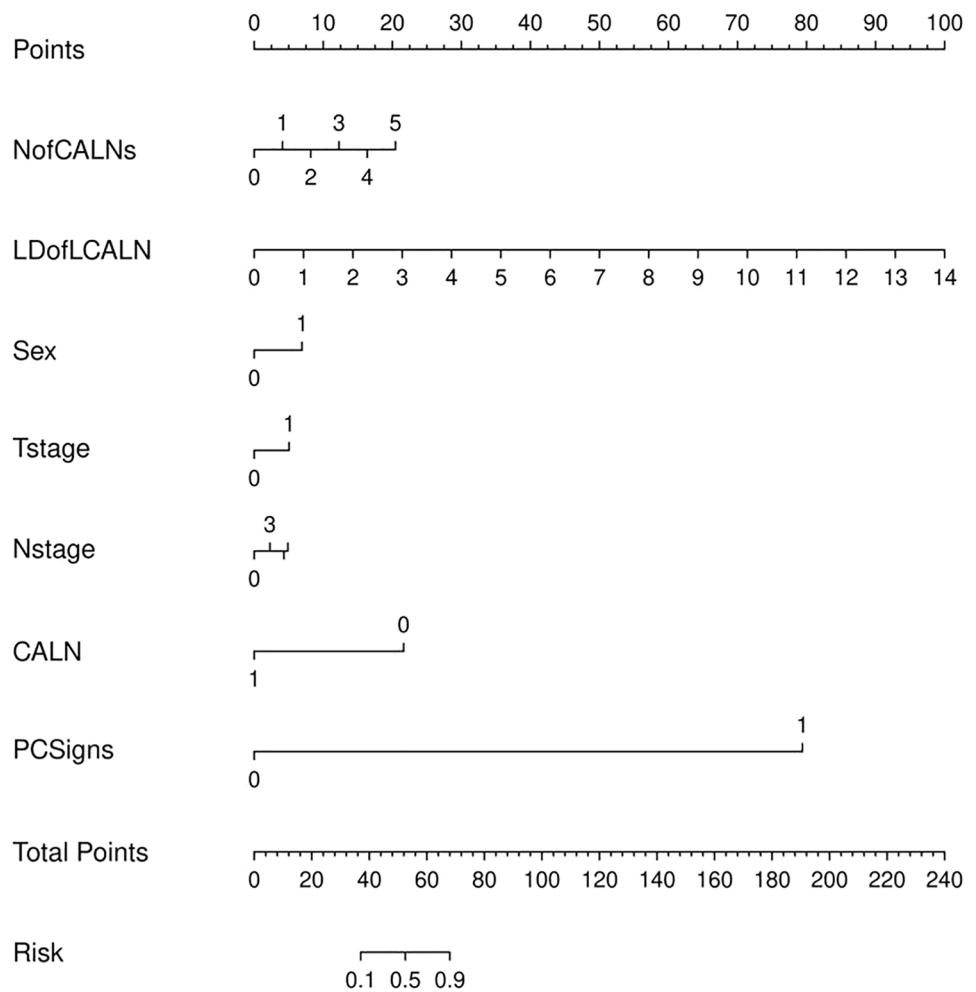
and helped make a more accurate treatment plan for GC patients.

The lymph node of the cardiophrenic angle was an important basis for clinical diagnosis and prognosis evaluation of tumors. Previous studies have shown that the cardiophrenic angle lymph node is an important predictor in the diagnosis and progression monitoring of digestive tract and ovarian malignant tumors [17–19]. Compared with the previous model, this study innovatively focused on the CT characteristics of CALN [22]. The diagnostic effectiveness of this study was similar to or even better than some imaging or machine learning models [5, 7, 23, 24]. The characteristics of CPLN were also analyzed in this study. Through the addition of quantitative indicators, the prediction effect of

the model had been greatly improved. Other studies on the CALN in ovarian cancer had also confirmed the significance of the size of the CALN in the diagnosis of PM [20, 21]. This revealed the significance of quantitative indicators in the evaluation of CALN.

As far as the scanning technique was concerned, the examination of CALN was simple and easy. The guidelines recommended a chest scan to check for lung metastasis [25]. The examination of the cardiophrenic angle could be completed at the same time. However, CT scanning of CALN did not need the injection of a contrast agent. And the CT image of CALN was displayed because of the natural background, so it was easy to measure. The boundary of the

Fig. 4 Gastric cancer patients' PM probability could be predicted using a nomogram. *CALN* cardiophrenic angle lymph node, *LDofLCALN* long diameter of the largest CALN, *NofCALNs* number of CALNs, *PCSigns* peritoneal carcinoma signs



cardiophrenic angle lymph node was clear, the shape was regular, and the measurement result was more reliable.

Several related research directions were pursued. There had been a gradual understanding of the molecular mechanism underlying gastric cancer peritoneal metastasis. A non-negligible role was played by lipid metabolism in epithelial-mesenchymal transition (EMT), which was crucial to gastric cancer metastasis [26]. A cancer cell's ability to metastasize was affected by the presence of collagen in its microenvironment [4]. The cardiophrenic lymph node was the relay station of lymphatic drainage, and the cardiophrenic lymph node could be enlarged due to tumors in patients with peritoneal metastasis. The relationship

between the molecular mechanism of GC peritoneal metastasis and CALN enlargement was worthy of further study. In addition, it was expected that the CALNs could be pathologically verified by cardiophrenic angle lymphadenectomy [27].

In our research, there were some limitations. Firstly, as a retrospective study conducted in a single subspecies center, it was not certain that it applies to all ethnic groups. Secondly, a slight increase in peritoneal fat density was not used as a feature of peritoneal metastasis because it might be suggestive but lacks specificity.

In conclusion, CALN could predict gastric cancer peritoneal metastasis. The model in this study provided a powerful

Fig. 5 The calibration plot of the nomogram model. The solid line is the bias-corrected line. The dashed lines represent the ideal line and the apparent line. There is excellent calibration evident from the calibration plot, which is close to the diagonal

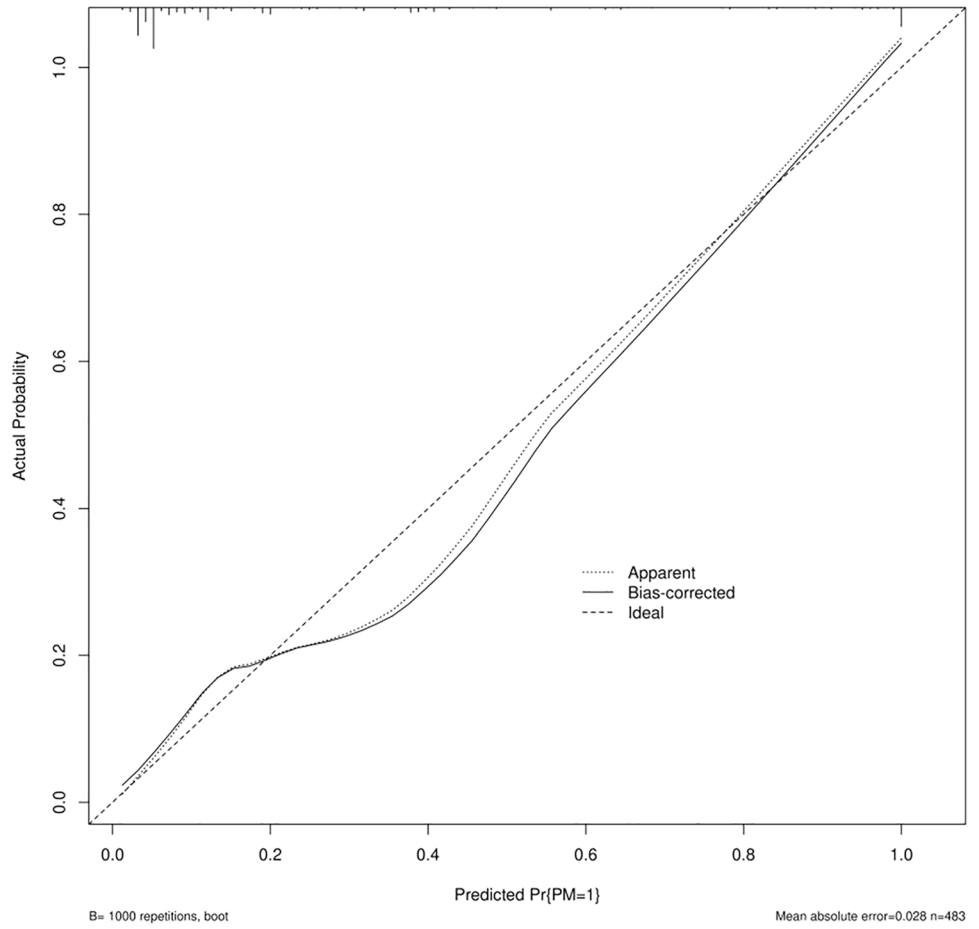
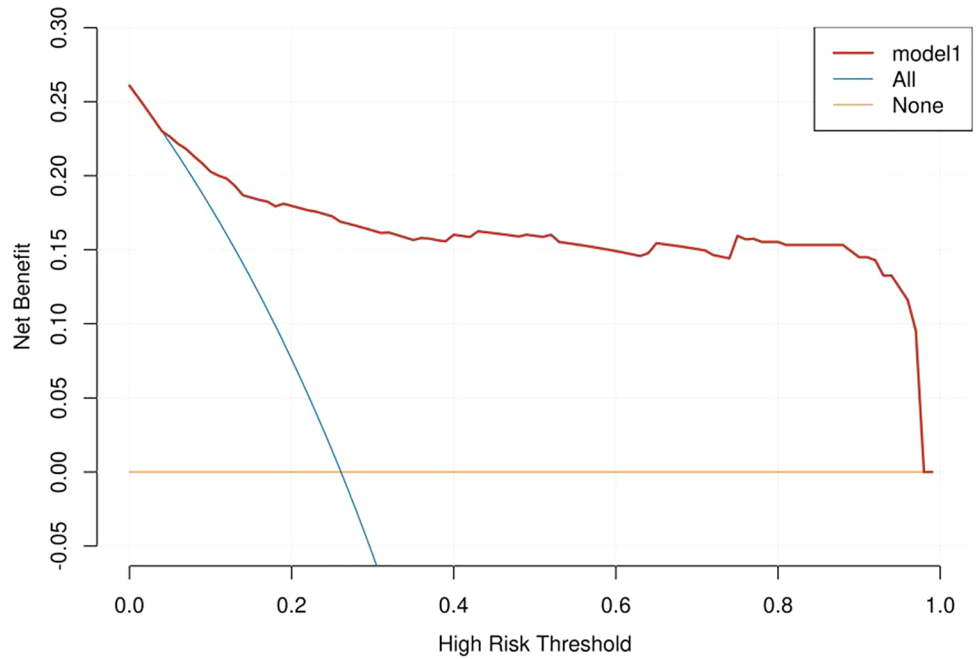


Fig. 6 DCA curve of the model. The model prediction effect is shown by the area under the curve



predictive tool for determining PM in GC patients and helping clinicians allocate treatment.

Supplementary Information The online version contains supplementary material available at <https://doi.org/10.1007/s00261-023-03848-7>.

Declarations

Conflict of interest The authors declare that there are no conflicts of interest to disclose in this study.

Open Access This article is licensed under a Creative Commons Attribution 4.0 International License, which permits use, sharing, adaptation, distribution and reproduction in any medium or format, as long as you give appropriate credit to the original author(s) and the source, provide a link to the Creative Commons licence, and indicate if changes were made. The images or other third party material in this article are included in the article's Creative Commons licence, unless indicated otherwise in a credit line to the material. If material is not included in the article's Creative Commons licence and your intended use is not permitted by statutory regulation or exceeds the permitted use, you will need to obtain permission directly from the copyright holder. To view a copy of this licence, visit <http://creativecommons.org/licenses/by/4.0/>.

References

- Sung H, Ferlay J, Siegel RL, Laversanne M, Soerjomataram I, Jemal A, Bray F. Global Cancer Statistics 2020: GLOBOCAN Estimates of Incidence and Mortality Worldwide for 36 Cancers in 185 Countries. *CA Cancer J Clin* 2021;71(3):209-249. doi: <https://doi.org/10.3322/caac.21660>
- Fujitani K, Yang HK, Mizusawa J, Kim YW, Terashima M, Han SU, Iwasaki Y, Hyung WJ, Takagane A, Park DJ, Yoshikawa T, Hahn S, Nakamura K, Park CH, Kurokawa Y, Bang YJ, Park BJ, Sasako M, Tsujinaka T, investigators R. Gastrectomy plus chemotherapy versus chemotherapy alone for advanced gastric cancer with a single non-curable factor (REGATTA): a phase 3, randomised controlled trial. *Lancet Oncol* 2016;17(3):309-318. doi: [https://doi.org/10.1016/S1470-2045\(15\)00553-7](https://doi.org/10.1016/S1470-2045(15)00553-7)
- Li ZY, Tang L, Li ZM, Li YL, Fu J, Zhang Y, Li XT, Ying XJ, Ji JF. Four-Point Computed Tomography Scores for Evaluation of Occult Peritoneal Metastasis in Patients with Gastric Cancer: A Region-to-Region Comparison with Staging Laparoscopy. *Ann Surg Oncol* 2020;27(4):1103-1109. doi: <https://doi.org/10.1245/s10434-019-07812-y>
- Chen D, Liu Z, Liu W, Fu M, Jiang W, Xu S, Wang G, Chen F, Lu J, Chen H, Dong X, Li G, Chen G, Zhuo S, Yan J. Predicting post-operative peritoneal metastasis in gastric cancer with serosal invasion using a collagen nomogram. *Nat Commun* 2021;12(1):179. doi: <https://doi.org/10.1038/s41467-020-20429-0>
- Dong D, Tang L, Li ZY, Fang MJ, Gao JB, Shan XH, Ying XJ, Sun YS, Fu J, Wang XX, Li LM, Li ZH, Zhang DF, Zhang Y, Li ZM, Shan F, Bu ZD, Tian J, Ji JF. Development and validation of an individualized nomogram to identify occult peritoneal metastasis in patients with advanced gastric cancer. *Ann Oncol* 2019;30(3):431-438. doi: <https://doi.org/10.1093/annonc/mdz001>
- Chen Y, Xi W, Yao W, Wang L, Xu Z, Wels M, Yuan F, Yan C, Zhang H. Dual-Energy Computed Tomography-Based Radiomics to Predict Peritoneal Metastasis in Gastric Cancer. *Front Oncol* 2021;11:659981. doi: <https://doi.org/10.3389/fonc.2021.659981>
- Huang W, Zhou K, Jiang Y, Chen C, Yuan Q, Han Z, Xie J, Yu S, Sun Z, Hu Y, Yu J, Liu H, Xiao R, Xu Y, Zhou Z, Li G. Radiomics Nomogram for Prediction of Peritoneal Metastasis in Patients With Gastric Cancer. *Front Oncol* 2020;10:1416. doi: <https://doi.org/10.3389/fonc.2020.01416>
- Wang L, Lv P, Xue Z, Chen L, Zheng B, Lin G, Lin W, Chen J, Xie J, Duan Q, Lu J. Novel CT based clinical nomogram comparable to radiomics model for identification of occult peritoneal metastasis in advanced gastric cancer. *Eur J Surg Oncol* 2022. doi: <https://doi.org/10.1016/j.ejso.2022.06.034>
- Jiang Y, Liang X, Wang W, Chen C, Yuan Q, Zhang X, Li N, Chen H, Yu J, Xie Y, Xu Y, Zhou Z, Li G, Li R. Noninvasive Prediction of Occult Peritoneal Metastasis in Gastric Cancer Using Deep Learning. *JAMA Netw Open* 2021;4(1):e2032269. doi: <https://doi.org/10.1001/jamanetworkopen.2020.32269>
- Mirniaharikandehi S, Heidari M, Danala G, Lakshmiarahan S, Zheng B. Applying a random projection algorithm to optimize machine learning model for predicting peritoneal metastasis in gastric cancer patients using CT images. *Comput Methods Programs Biomed* 2021;200:105937. doi: <https://doi.org/10.1016/j.cmpb.2021.105937>
- Borggreve AS, Goense L, Brenkman HJF, Mook S, Meijer GJ, Wessels FJ, Verheij M, Jansen EPM, van Hillegersberg R, van Rossum PSN, Ruurda JP. Imaging strategies in the management of gastric cancer: current role and future potential of MRI. *Br J Radiol* 2019;92(1097):20181044. doi: <https://doi.org/10.1259/bjr.20181044>
- Lin CN, Huang WS, Huang TH, Chen CY, Huang CY, Wang TY, Liao YS, Lee LW. Adding Value of MRI over CT in Predicting Peritoneal Cancer Index and Completeness of Cytoreduction. *Diagnostics (Basel)* 2021;11(4). doi: <https://doi.org/10.3390/diagnostics11040674>
- De Vuysere S, Vandecaveye V, De Bruecker Y, Carton S, Vermeiren K, Tollens T, De Keyzer F, Dresen RC. Accuracy of whole-body diffusion-weighted MRI (WB-DWI/MRI) in diagnosis, staging and follow-up of gastric cancer, in comparison to CT: a pilot study. *BMC Med Imaging* 2021;21(1):18. doi: <https://doi.org/10.1186/s12880-021-00550-2>
- Fu L, Huang S, Wu H, Dong Y, Xie F, Wu R, Zhou K, Tang G, Zhou W. Superiority of [(68)Ga]Ga-FAPI-04/[(18)F]FAPI-42 PET/CT to [(18)F]FDG PET/CT in delineating the primary tumor and peritoneal metastasis in initial gastric cancer. *Eur Radiol* 2022;32(9):6281-6290. doi: <https://doi.org/10.1007/s00330-022-08743-1>
- Xue B, Jiang J, Chen L, Wu S, Zheng X, Zheng X, Tang K. Development and Validation of a Radiomics Model Based on (18)F-FDG PET of Primary Gastric Cancer for Predicting Peritoneal Metastasis. *Front Oncol* 2021;11:740111. doi: <https://doi.org/10.3389/fonc.2021.740111>
- Caspers IA, Sikorska K, Slaughter AE, van Amelsfoort RM, Meershoek-Klein Kranenbarg E, van de Velde CJH, Lind P, Nordmark M, Jansen EPM, Verheij M, van Sandick JW, Cats A, van Grieken NCT. Risk Factors for Metachronous Isolated Peritoneal Metastasis after Preoperative Chemotherapy and Potentially Curative Gastric Cancer Resection: Results from the CRITICS Trial. *Cancers (Basel)* 2021;13(18). doi: <https://doi.org/10.3390/cancers13184626>
- Caramella C, Pottier E, Borget I, Malka D, Goere D, Boige V, Honore C, Dartigues P, Dumont F, Ducreux M, Elias D, Dromain C. Value of cardiophrenic angle lymph node for the diagnosis of colorectal peritoneal carcinomatosis. *Eur J Cancer* 2013;49(18):3798-3805. doi: <https://doi.org/10.1016/j.ejca.2013.06.044>
- Jeune F, Brouquet A, Caramella C, Gayet M, Abdalla S, Verin AL, Thiroit Bidault A, Penna C, Benoist S. Cardiophrenic angle lymph node is an indicator of metastatic spread but not specifically peritoneal carcinomatosis in colorectal cancer patients: Results of a prospective validation study in 91 patients. *Eur J*

- Surg Oncol 2016;42(6):861-868. doi: <https://doi.org/10.1016/j.ejso.2016.02.256>
19. Oommen I, Chandramohan A, Raji PS, Thomas A, Joel A, Samuel Ram T, Peedicayil A. Clinical significance of CT detected enlarged cardiophrenic nodes in ovarian cancer patients. *Abdom Radiol (NY)* 2021;46(1):331-340. doi: <https://doi.org/10.1007/s00261-020-02618-z>
 20. Luger AK, Steinkohl F, Aigner F, Jaschke W, Marth C, Zeimet AG, Reimer D. Enlarged cardiophrenic lymph nodes predict disease involvement of the upper abdomen and the outcome of primary surgical debulking in advanced ovarian cancer. *Acta Obstet Gynecol Scand* 2020;99(8):1092-1099. doi: <https://doi.org/10.1111/aogs.13835>
 21. Addley S, Asher V, Kirke R, Bali A, Abdul S, Phillips A. What are the implications of radiologically abnormal cardiophrenic lymph nodes in advanced ovarian cancer? An analysis of tumour burden, surgical complexity, same-site recurrence and overall survival. *Eur J Surg Oncol* 2022. doi: <https://doi.org/10.1016/j.ejso.2022.06.006>
 22. Kim M, Jeong WK, Lim S, Sohn TS, Bae JM, Sohn IS. Gastric cancer: development and validation of a CT-based model to predict peritoneal metastasis. *Acta Radiol* 2020;61(6):732-742. doi: <https://doi.org/10.1177/0284185119882662>
 23. Liu S, He J, Liu S, Ji C, Guan W, Chen L, Guan Y, Yang X, Zhou Z. Radiomics analysis using contrast-enhanced CT for preoperative prediction of occult peritoneal metastasis in advanced gastric cancer. *Eur Radiol* 2020;30(1):239-246. doi: <https://doi.org/10.1007/s00330-019-06368-5>
 24. Wang L, Lv P, Xue Z, Chen L, Zheng B, Lin G, Lin W, Chen J, Xie J, Duan Q, Lu J. Novel CT based clinical nomogram comparable to radiomics model for identification of occult peritoneal metastasis in advanced gastric cancer. *Eur J Surg Oncol* 2022;48(10):2166-2173. doi: <https://doi.org/10.1016/j.ejso.2022.06.034>
 25. Amin MB, Greene FL, Edge SB, Compton CC, Gershenwald JE, Brookland RK, Meyer L, Gress DM, Byrd DR, Winchester DP. The Eighth Edition AJCC Cancer Staging Manual: Continuing to build a bridge from a population-based to a more "personalized" approach to cancer staging. *CA Cancer J Clin* 2017;67(2):93-99. doi: <https://doi.org/10.3322/caac.21388>
 26. Wang C, Yang Z, Xu E, Shen X, Wang X, Li Z, Yu H, Chen K, Hu Q, Xia X, Liu S, Guan W. Apolipoprotein C-II induces EMT to promote gastric cancer peritoneal metastasis via PI3K/AKT/mTOR pathway. *Clin Transl Med* 2021;11(8):e522. doi: <https://doi.org/10.1002/ctm2.522>
 27. Acs M, Piso P, Prader S. Current Status of Metastatic Cardiophrenic Lymph Nodes (CPLNs) in Patients With Ovarian Cancer: A Review. *Anticancer Res* 2022;42(1):13-24. doi: <https://doi.org/10.21873/anticancer.15452>

Publisher's Note Springer Nature remains neutral with regard to jurisdictional claims in published maps and institutional affiliations.